Unloading Effect of the Shear Resistance of Rock Joints

Jianan Yang
Peoples Liberation Army Engineering University
Shuo Wang
Naval Coastal Defense Engineering Brigade of the Northern Thearter
Qiongting Wang
Xiangtan University
Wenzheng Xing
Peoples Liberation Army Engineering University
Pengxian Fan (fan-px@139.com)
Peoples Liberation Army Engineering University

Research Article

Keywords: rock joints, direct shear test, shear resistance, unloading effect, joint roughness coefficient

Posted Date: October 29th, 2021

DOI: https://doi.org/10.21203/rs.3.rs-948793/v1

Abstract

To investigate the stress path dependent of rock joints, a comparative experimental study was conducted using cement mortar replicas of artificially split rock joints. In total, 32 replicas were casted and divided into four groups by joint roughness coefficient (JRC). The effects of morphologic characteristics, normal stress levels and stress paths on the shear strength of joints were investigated through tangential loading tests and normal unloading tests. The comparative analysis on the test results indicated that the shear resistance has a distinct unloading effect. The variation trend of shear/normal stress ratio against the normal stress and JRC of the two test conditions were identical. However, under low normal-stress condition, the stress ratio of the joints under normal unloading stress is the higher one; while under higher normal stress, the relationship becomes converse. Compared to that of the tangential loading condition, shear/normal stress ratio of the unloading stress path reduces rapidly as the increasing of normal stress, and the influence of the morphology is masked under lower normal stress. The comparative study revealed a previously unknown unloading effect on the mechanical behavior of rock joints and will aid the estimation of the rock joints' stability in a complex stress environment.

1. Introduction

A natural rock mass contains numerous structural planes from faults, joints to microcracks. These structural planes of different sizes can greatly affect the stability of natural or engineered rock structures (Barton 2013). Due to the control role on the safety of rock engineering, the mechanical performance of rock joints is one of the hottest topics in field of rock mechanics and rock engineering.

In the excavation of underground engineering, the stress of specific direction will be unloaded. The reduction in the normal stress of the structural plane may easily cause serious engineering disasters, such as unloading splitting of wall rock and structural controlled rockburst. Particularly, in situations involving large depths and high initial in situ stress, the structural plane is a weak plane that affects and controls the form of failure and the damage severity of the wall rock (Liu et al. 2016). Estimating the shear resistance of natural rock discontinuities under unloading circumstance is crucial for the stability analysis and support design in rock engineering.

The rockburst accident of the diversion tunnel of Jinping II hydropower station is an example of such a disaster. Owing to the unloading of the normal stress of a rigid fault, the stress redistribution during chamber excavation led to a serious tectonic rockburst and great economic loss (Zhang et al. 2012, 2013). In the case of the Baihetan underground caverns, the contact shear slip of highly stressed staggered zones is one of the main failure mode under conditions of excavation unloading disturbs (Duan et al. 2017).

According to literatures (Zhou et al. 2016; Meng et al. 2019; Zhou et al. 2019; Han et al. 2020; Hu et al. 2020; Li, B. et al. 2020; Li, Y. C. et al. 2020), the shear resistance and stability of rock mass discontinuity is mainly controlled by three factors, namely, the morphology of discontinuity, the normal stress level of the

joint and strength characteristics of materials. Considering that the basic friction parameters of materials and asperities before losing shear stability is commonly assumed to be constant, the shear performance of a structural plane or rock joint is governed by the coupling between the normal and shear stresses. A higher normal stress is favourable for improving the shear capacity of a structural plane. When a sufficiently high normal stress is applied, the joint maintains its shear stability.

However, if the normal stress is unloaded to a relatively low level, the rock joint that is subjected to shear may fail. Experiments and in situ observations have already indicated that the mechanical and deformation performance of rock mass is obviously influenced by the stress path (Fan et al. 2018; Li et al. 2019; You 2020). At the same time, the unloading effect on the rock joints' shear resistance has not been well investigated. The major of the existing researches on the behaviour of the rock discontinuities focused on the peak shear resistance under tangential loading conditions. Literatures devoted on the unloading effect of rock joints or jointed rocks are relatively rare, and most of the works are qualitative.

Zhu and Huang (2019) investigated the shear mechanics characteristics of the rock under unloading conditions, and described the relationship between the initial normal stress and the failure normal stress by using the exponential model. Zhou et al. (2003) explored the mechanical characteristics of a fractured rock mass under loading and unloading conditions, proposed the stress intensity factors of each stage and analysed the similarities and differences of stress intensity factors under loading and unloading conditions. Huang et al. (2020) studied the shear mechanical properties of rock mass with single prefabricated crack during unloading, established five failure modes of fractured rock mass through analysis of crack propagation and mechanical properties. Zhang et al. (2009) explored the change in the mechanical properties of structural planes in the unloading state, and they found that the climbing effect is more sufficient due to normal unloading. Through in situ investigation, Yin et al. (2021) studied the shear behavior of fractured rock mass under different initial shear stress and normal stress unloading and found that high shear stress will promote dilatancy deformation, while high normal stress will inhibit dilatancy deformation. Zhu et al. (2020) studied the shear mechanical properties of rock mass with parallel pre-faults during unloading, and found that the fracture surface of unloading test is less damaged than that of direct shear test. Chen et al. (2018) experimentally investigated the influence of jointed rock bridge on the bearing capacity and failure mode of rock slopes under excavation unloading and found that the unloading failure is more brittle compared with uniaxial loading. Through in situ investigation, Li et al. (2017) investigated the failure process of the surrounding rock during excavation and found that the unloading results from excavation induced numerous microseismic events. Tu and Deng (2021) through the geological survey of the Southwest River Valley, considered that the unloading effect caused by the rapid river cutting affected the deep collapse failure of the rock mass, and proposed an empirical method that estimated tensile unloading depths of a rock masses.

Up to now, the influence and mechanism of normal unloading on the shear performance of rock joints are still unclear. In this study, a total 32 replicas of artificially split rock joints were casted and tested by direct shear apparatus. Among them, 16 samples were tested under tangential loading stress path, and the rest 16 samples, were tested under normal-stress unloading stress path. A comparative study of the

tangential loading (with fixed normal-stress levels) and normal unloading tests (with fixed tangential stress levels) was conducted. The experiment results revealed a considerable stress-path effect of the shear performance of rock joints.

2. Sample Preparation

Four groups of structural planes, namely, S1 to S4, were prepared through splitting tests of granite cuboids. In order to ensure the repeatability, cement mortar was used as the analogue material for rocks.

The joints samples were prepared following the next procedure. Firstly, model gypsum was poured on one of the surface of the prototype joint. As the gypsum solidified, the characteristics of the surface were reproduced. Thereafter, cement mortar was poured on the gypsum moulds to reproduce the replicas of the surfaces of prototype rock joints. This procedure was repeated until sufficient replicas were produced.

In total, 32 artificial joints of dimensions 200×100×100 mm were casted. At the same times, standard cubic samples (100×100×100 mm) also were prepared for determining the basic material parameters.

The results of the splitting test and the uniaxial compression test indicate that the average tension strength and compression strength of the analogue material were 2.10 MPa and 40.82 MPa, respectively. The basic friction angle of the prepared materials was determined as 32° by a tilt test.

In order to examine the accuracy of the replicas, a fidelity analysis was conducted (Jiang et al. 2018). Five cement mortar samples were randomly selected, and the morphological features of the structural surfaces were scanned by a 3D scanner. The scanning accuracy is 0.2 mm. Then, the morphological characteristics of the original surface of the rock joints and its cement mortar replicas were compared by using 3D point cloud processing software Cloudcompare. The fidelity analysis results show that the average fidelity of the replicas exceeds 98.4%, indicating a very good reproduction quality and uniformity.

The quantification of surface roughness has taken many different forms (Magsipoc et al. 2020). The joint roughness coefficient (JRC) is a widely used two-dimensional surface roughness characterisation parameter which provides a simple and objective index of surface morphology (Barton 1978). In this study, the JRC was determined from the average value of ten evenly spaced profiles of the surface. The root mean square of the slope, proposed by Tes and Cruden (1979), was adopted to calculate the roughness values of the four groups of the joints replicas. The calculated JRCs are listed in the following Table 1.

Table 1 The calculated JRC of the artificial joints

	S1	S2	S3	S4
JRC	7.02	7.97	8.22	11.02

3. Test Procedure

The tests were carried out on a microcomputer controlled electronic rock direct shear apparatus. The apparatus comprised a loading device, a microcomputer servo control system, a stress–strain measuring device, etc. The test equipment could be controlled in the force or displacement mode. The tangential loading capacity was 1000 kN, and the normal loading capacity was 300 kN.

In the conventional direct shear tests, the normal load was controlled by force, while the tangential load was controlled by displacement. and the tangential loading speed was 0.02 mm/s. The tangential load was loaded several seconds after the normal load reached the target value. Four levels of normal stress—1.0, 3.0, 5.0 and 10.0 MPa—were considered in the shear stress loading tests.

In the normal stress unloading tests, both the normal and tangential loads were controlled by force. First, the normal and tangential stresses were loaded to the pre-determined value successively, and then, the normal stress is unloaded step by step. During the unloading process, only the normal load was reduced, while the tangential load force was maintained constant. The specimen was considered to have failed when the tangential force decreased and the tangential displacement increased rapidly. The test will be terminated when the joint fails.

The tangential loading speed was 0.2 kN/s, and the target value of the tangential load varied with the initial normal stress. After the tangential load reached the target value for a certain period of time, normal unloading was performed in steps of -0.4 kN/s. Under each normal-stress level, the difference in the normal unloading steps and the holding time after reaching the target value are identical. The conceptual stress path of the samples is shown in Fig.1.

The initial shear force (or stress) of the unloading test is selected according to the shear resistance peak of the conventional loading test. To avoid joint failures before the unloading procedure starts, the initial shear stress was set as 60–80% of the peak value of shear resistance determined according to the results of loading tests. The difference of the normal stress at each level was selected according to the initial normal stress. The parameters of the normal stress unloading tests are given in Table 2.

Table 2 The settings of normal stress of the unloading tests

Initial normal stress (MPa)	Initial shear stress (MPa)	Unloading step (MPa)	Holding time (s)
1.0	0.75	0.05	40
3.0	2.00	0.20	40
5.0	3.00	0.25	40
10.0	4.75	0.25	35

During the test, the time, normal force, normal deformation, normal displacement, tangential force, tangential deformation and tangential displacement were collected by displacement sensors and servo

control system.

When the normal stress equals to 10 MPa, the total tangential loading time and normal unloading time were relatively long, and the structural plane tended to be damaged during the pre-loading stage. Therefore, the holding time of each step unloading was set relatively small.

4. Test Results

4.1 Results of shear tests under the normal-stress unloading condition

The typical stress–time curves and displacement–time curves obtained from the conducted normal-stress unloading tests are given in Fig.2.

From Fig. 2, a general deformation mode of the normal-stress unloading test can be found. The shear displacement of the joints increases linearly as the shear stress increases from zero to the pre-determined value, and then, it remains stable. When the normal stress is unloaded stepwise, the shear deformation increases gradually. If the normal stress is unloaded to a critical value below which the joint can't resist the pre-loaded shear stress, the joint fails, and the shear displacement increases rapidly and loses its stability. Meanwhile, the shear stress will decrease.

The critical displacement for joints under different initial normal-stress conditions ranges from 1 to 6 mm. The joints with the least JRC (S1 group) have the largest critical displacements. A joint with higher JRC tends to endure larger critical displacement. However, the JRC and critical displacement are weakly correlated.

The critical normal stresses under which the joints lose their stability are listed in Table 3.

Here, note that the unloading test of S3 group under 5.0 MPa initial normal stress was a trial test to determine the appropriate test settings. The normal-stress holding time of the specimen was 60 seconds, which is longer than that of the other specimens. Because of the different test settings, the corresponding result, i.e., 3.78 MPa, is excluded as an outlier in the following analysis and regressions.

Table 3 Critical normal stress of unloading tests

Initial normal stress (MPa)	Shear stress (MPa)	Critical normal stress when joints fail（MPa）			
		S1	S2	S3	S4
1.0	0.75	0.55	0.61	0.70	0.80
3.0	2.00	1.67	1.86	2.05	2.10
5.0	3.00	2.82	3.41	~~3.78~~	3.54
10.0	4.75	5.03	5.26	5.54	5.65

The data in Table 3 indicates that the larger the shear stress, the higher is the critical normal stress. Under identical initial normal stresses, the critical normal stress of complex joints (S3 and S4) is lower than that of simple joints (S1 and S2), and the shear resistance of complex joints are higher than that of simple joints when the other conditions are the same.

In the normal stress unloading test, under the condition of low normal stress, the shear strength is higher than the applied normal stress. If the normal stress increases to high stress domain, the peak value of shear resistance is lower than the normal stress.

4.2 Unloading effect of shear resistance and influence of morphology

According to the data of loading and unloading tests, Fig. 3 shows the relationship between the normal stress and shear resistance.

Fig. 3 indicates that the shear resistance of joints increases approximately linearly with increasing surface complexity and normal stress, both for the shear loading stress path and normal unloading stress path. However, the data points are very closely distributed, and it is difficult to perform a detailed analysis.

To compare the results of loading and unloading paths intuitively, a non-dimensional index, namely, the stress ratio, was defined. For the loading cases, the stress ratio was defined as the ratio of the shear strength to the pre-determined normal stress, and for the unloading cases, it was defined as the ratio of the pre-determined shear stress to the critical normal stress corresponding to the failure of the joint.

The stress ratios are listed in Table 4.

Table 4 Stress ratios for loading and unloading

	Shear stress loading					Normal-stress unloading				
	Normal stress(MPa)					Initial normal stress(MPa)				
	1.0	3.0	5.0	10.0	Average	1.0	3.0	5.0	10.0	Average
S1	0.83	0.83	0.81	0.76	0.81	0.94	0.95	0.85	0.84	0.90
S2	0.94	0.84	0.93	0.74	0.86	1.07	1.07	0.88	0.86	0.97
S3	1.06	1.02	0.98	0.77	0.96	1.25	0.98	~~0.79*~~	0.90	1.04
S4	1.21	1.15	0.99	0.81	1.04	1.36	1.20	1.06	0.94	1.14
Average	1.01	0.96	0.93	0.77	/	1.12	1.05	0.93	0.89	/

*the data is abnormal and not included in the following analysis.

From the results listed in Table 4, the following observations are made:

(1) The stress ratio of joints decreases as the normal stress increases. Under tangential loading stress, the highest stress ratio is 1.21, corresponding to the case of the lowest normal stress, and the lowest stress ratio is 0.74, corresponding to the case of the highest normal stress. As the normal stress increases from 1.0 MPa to 10.0 MPa, the average stress ratio of the joints decreases from 1.01 to 0.77, which is a reduction of about 24%. Under normal unloading stress, when the normal stress increases from 1.0 MPa to 10.0 MPa, the average stress ratio of joints decreases from 1.12 to 0.89, which is a reduction of about 21%.

(2) The stress ratio of joints increases with the complexity of the surface morphology of the joints. Under tangential loading stress, the highest stress ratio is 1.21, corresponding to the case of the joint with the highest JRC, while the lowest stress ratio is 0.74, corresponding to the case of the joint with the second-lowest JRC (which is very close to the stress ratio of the joint with the lowest JRC). As the JRC increases from 7.02 (S1) to 11.02 (S4), the average stress ratio of joints increases from 0.81 to 1.04 by about 28%. Under normal unloading stress, when the normal stress increases from 7.02 (S1) to 11.02 (S4), the average stress ratio of joints increases from 0.90 to 1.14 by about 27%.

4.3 Effect of stress path on shear strength

The variations in the stress ratio under the loading and unloading stress paths are quite similar. However, because failure cannot be predicted in the normal stress unloading tests, hence, the stress ratios of the loading tests and unloading tests cannot be compared directly owing to the un-uniform normal stress levels.

In order to reveal the variation tendency of the shear resistance of joints, the non-dimensional stress ratios were linearly regressed according to the normal stress. The regression results are shown in Fig.4.

Fig.4 shows that the relationship between the stress ratio and normal stress can be described by lines with negative slopes. The lowest correlation index R is 0.812, and half of the indices are larger than 0.95, indicating strong linear correlation between the regression parameters.

The slopes of the regression lines are closely related to the morphology of the joint surface. From S1 to S4, the slopes of the regression lines decrease from -0.008 to -0.046, while under normal unloading condition, the slopes decrease from -0.025 to -0.092. The more complex the morphology, the faster does the stress ratio decrease with the normal stress.

Since the stress ratio of joint with higher roughness has a larger descending rate, the regression lines gradually come closer to each other as the normal stress increases. It rational to speculate that they will converge to one point or approach a certain limitation, under both tangential loading and normal unloading conditions. In other words, the influence of joint morphology weakens as the normal stress increases, and if the normal stress is sufficiently high, the influence of joints morphology tends to disappear.

In order to intuitively compare the variations in stress ratios and reveal the unloading effect, the regression lines were plotted in one coordinate system, as shown in Fig.5

From Fig.5, one can see that the stress ratio decreases with an increase in the normal stress for both tangential loading stress path and normal unloading stress path. Under low normal stress condition, the stress ratios of joints under the normal unloading stress path are significantly higher (about 10%) than those of the joints under the tangential loading stress path. However, the stress ratios of the joints under the normal unloading stress path decrease more rapidly as the normal stress increases. Therefore, when the normal stress is higher, the relationship is reversed; in other words, the stress ratios of joints under tangential loading are greater than those of the joints under normal unloading. Compared to the joints under tangential loading, those under the unloading stress experience lower normal stress such that the influence of the joint morphology is totally masked. The intersection of the regression lines of the stress ratios of joints under tangential loading is larger than 10 MPa, and the corresponding values are estimated as 5.5–6.0 MPa.

According to the comparative analysis, the shear strength of rock joints has an obvious unloading effect. This stress-path dependence has not been well investigated and the mechanism is still not clear. A comparison of the joint surface morphology before and after the action of normal stress leads us to the deduction that the stress-path dependence of joints arises partly from the imperfect matching of the two surfaces of one joint, which is likely to cause the damage of asperities during normal stress loading.

In order to verify this conjecture, two normal loading tests (purely loaded by normal stress and without any shearing) were conducted to compare the variations in the joint surface morphology before and after the action of normal stress. The joint surfaces after the action of 10.0 MPa normal stress were scanned by the 3D scanner. The scanning accuracy was selected as 0.1 mm. The comparison results are shown in Fig.6.

As seen from Fig. 6, only about 94% of the data points of sample 1 were unaffected by the normal loading process, and about 96% of the data points of sample 2 were unaffected. The damage of joint surface asperities weakens the influence of the initial morphology and may result in an earlier convergence of the regression lines.

5. Conclusion

In order to investigate the behaviour of rock joints under normal unloading stress, a comparative experimental study was conducted using cement mortar replicas of artificially split rock joints. The effects of normal stress, morphologic characteristics and stress paths on shear strength were investigated by performing tangential loading tests with pre-determined normal stress and normal unloading tests with pre-determined shear stress. From the results, the following conclusions were drawn:

(1) The shear strength or resistance of joints increases approximately linearly as the normal stress and JRC increase, under both tangential loading and normal unloading conditions. The relationship between

the stress ratio and normal stress can be described by a bunch of lines with negative slopes' instead, showing a decrease toward the high normal stress zone. The slopes of the regression lines decrease as the complexity of joint surfaces increases.

(2) Although the variation trends of the stress ratio against normal stress and JRC under the two test conditions are similar, a notable unloading effect is observed.

(3) Under the low normal-stress condition, the stress ratios of joints of the normal unloading stress path are higher than those of the joints subjected to the tangential loading stress path. The stress ratios of the joints subjected to the normal unloading stress path decrease more rapidly as the normal stress increases. Therefore, when the normal stress is high, the relationship is reversed.

(4) Under unloading stress, the normal stress decreases, thereby completely masking the influence of the joint morphology. The estimated intersection of the regression lines of stress ratio of joint decreases from >10 MPa to about 5.5–6.0 MPa.

Declarations

Acknowledgements

The authors gratefully acknowledge the support of the National Natural Science Foundation of China (No. 51979280).

Funding

Partial financial support was received from the National Natural Science Foundation of China (No. 51979280).

Conflict of interest

On behalf of all authors, the corresponding author states that there is no conflict of interest.

Availability of data and material

The datasets used or analysed during the current study are available from the corresponding author on reasonable request.

Code availability

Not applicable.

Authors' contributions

All authors contributed to the study conception and design. Material preparation, data collection and analysis were performed by Jianan Yang, Shuo Wang, Qiongting Wang, Wenzheng Xing and Pengxian

Fan. The first draft of the manuscript was written by Pengxian Fan and all authors commented on previous versions of the manuscript. All authors read and approved the final manuscript.

Ethics approval

Not applicable.

Consent to participate

Not applicable.

Consent for publication

Not applicable.

References

Barton N (1978) Suggested methods for the quantitative description of discontinuities in rock masses. International Journal of Rock Mechanics and Mining Sciences, 15(6),319-368.

Barton N (2013) Shear strength criteria for rock, rock joints, rockfill and rock masses: Problems and some solutions. Journal of Rock Mechanics and Geotechnical Engineering, 5(4), 249-261. https://doi.org/10.1016/j.jrmge.2013.05.008.

Chen GQ, Liu D, Xu P et al (2018) True-triaxial test on unloading failure of jointed rock bridge. Chinese Journal of Rock Mechanics and Engineering, (02), 325-338. https://doi.org/10.13722/j.cnki.jrme.2017.0648.

Duan SQ, Feng XT, Jiang Q et al (2017) Failure modes and mechanisms for rock masses with staggered zones of Baihetan underground caverns under high geostress. Chinese Journal of Rock Mechanics and Engineering, 36(4), 852-864. https://doi.org/10.13722/j.cnki.jrme.2015.1236.

Fan PX, Li Y, Zhao YT et al (2018) Experimental study on unloading failure strength of red sandstone. Chinese Journal of Rock Mechanics and Engineering, 37, 852-861. https://doi.org/10.13722/j.cnki.jrme.2017.1368.

Han GS, Jing HW, Jiang YJ et al (2020) Effect of cyclic loading on the shear behaviours of both unfilled and infilled rough rock joints under constant normal stiffness conditions. Rock Mechanics and Rock Engineering, 53(1), 31-57. https://doi.org/10.1007/s00603-019-01866-w.

Hu J, Li SC, Liu HL et al (2020) New modified model for estimating the peak shear strength of rock mass containing nonconsecutive joint based on a simulated experiment. International Journal of Geomechanics, 20(7), 04020091. https://doi.org/10.1061/(ASCE)GM.1943-5622.0001732.

Huang D, Guo YQ, Cen DF et al (2020) Experimental investigation on shear mechanical behavior of sandstone containing a pre-existing flaw under unloading normal stress with constant shear stress. Rock Mechanics and Rock Engineering, 53(8), 3779-3792. https://doi.org/10.1007/s00603-020-02136-w.

Jiang Q, Yang B, Liu C et al.(2018) Manufacturing of natural rock joints by engraving and analysis of wearing damage of natural rock joints under shear tests. Chinese Journal of Rock Mechanics and Engineering, 37(11), 59-69. https://doi.org/10.13722/j.cnki.jrme.2018.0668.

Li A, Dai F, Xu N et al (2017) Failure mechanism and mode of surrounding rock of underground powerhouse at the right bank of Wudongde hydropower station subjected to excavation. Chinese Journal of Rock Mechanics and Engineering, 36(4), 781-793. https://doi.org/10.13722/j.cnki.jrme.2016.0691.

Li B, Ye XN, Dou ZH et al (2020) Shear strength of rock fractures under dry, surface wet and saturated conditions. Rock Mechanics and Rock Engineering, 53:2605–2622. https://doi.org/10.1007/s00603-020-02061-y.

Li J, Fan PX, Wang MY (2019) The stress conditions of rock core disking based on an energy analysis. Rock Mechanics and Rock Engineering, 52(2), 465-470. https://doi.org/10.1007/s00603-018-1634-7.

Li YC, Tang CA, Li DQ et al (2020) A new shear strength criterion of three-dimensional rock joints. Rock Mechanics and Rock Engineering, 53(3), 1477-1483. https://doi.org/10.1007/s00603-019-01976-5.

Liu GF, Feng XT, Jiang Q et al (2016) Failure characteristics, laws and mechanisms of rock spalling in excavation of large-scale underground powerhouse caverns in Baihetan. Chinese Journal of Rock Mechanics and Engineering, 35(5), 865-878. https://doi.org/10.13722/j.cnki.jrme.2015.0933.

Magsipoc E, Zhao Q, Grasselli G (2020) 2D and 3D roughness characterization. Rock Mechanics and Rock Engineering, 53, 1495–1519. https://doi.org/10.1007/s00603-019-01977-4.

Meng FZ, Wong LNY, Zhou H et al (2019) Shear rate effects on the post-peak shear behaviour and acoustic emission characteristics of artificially split granite joints. Rock Mechanics and Rock Engineering, 52(7), 2155-2174. https://doi.org/10.1007/s00603-018-1722-8.

Tse R, Cruden DM (1979) Estimating joint roughness coefficients. International Journal of Rock Mechanics & Mining Sciences & Geomechanics Abstracts, 16(5), 303-307. https://doi.org/10.1016/0148-9062(79)90241-9.

Tu GX, Deng, H (2021) Unloading depth of rock masses and its relations with river downcutting in deep valleys in Southwest China. Engineering Geology, 288, 106161. https://doi.org/10.1016/j.enggeo.2021.106161.

Yin ZM, Liu XR, Yang ZP et al (2021) Shear Behavior of Marlstone Containing Parallel Fissure under Normal Unloading. KSCE Journal of Civil Engineering, 25(4), 1283-1294. https://doi.org/10.1007/s12205-021-0959-z.

You MQ (2002) Strength and deformation of rock under complex loading path. Chinese Journal of Rock Mechanics and Engineering, 21(1), 23-28.

Zhang CQ, Feng XT, Zhou H et al (2012) Case histories of four extremely intense rockbursts in deep tunnels. Rock mechanics and rock engineering, 45(3), 275-288. https://doi.org/10.1007/s00603-011-0218-6.

Zhang CQ, Feng XT, Zhou H et al (2013) Rockmass damage development following two extremely intense rockbursts in deep tunnels at Jinping II hydropower station, southwestern China. Bulletin of engineering geology and the environment, 72(2), 237-247. https://doi.org/10.1007/s10064-013-0470-y.

Zhang QZ, Shen MR, Zhang LB (2009) Study on mechanical properties of rock discontinuity during unloading. Chinese Journal of Underground Space and Engineering, (06), 1126-1130+1137.

Zhong Z, Huang D, Zhang YF et al (2020) Experimental study on the effects of unloading normal stress on shear mechanical behaviour of sandstone containing a parallel fissure pair. Rock Mechanics and Rock Engineering, 53(4), 1647-1663. https://doi.org/10.1007/s00603-019-01997-0.

Zhou H, Meng FZ, Zhang CQ et al (2016) Investigation of the acoustic emission characteristics of artificial saw-tooth joints under shearing condition. Acta Geotechnica, 11(4), 925-939. https://doi.org/10.1007/s11440-014-0359-3.

Zhou H, Cheng GT, Zhu Y et al (2019) Experimental study of shear deformation characteristics of marble dentate joints. Rock and Soil Mechanics, 40(3), 852-860. https://doi.org/10.16285/j.rsm.2017.0964.

Zhou XP, Zhang YX, Ha QL (2003) Study on the stress intensity factor for the crack tips under unloading and loading. Underground Space, 23(2), 277-280.

Zhu TT, Huang D (2019) Experimental investigation of the shear mechanical behavior of sandstone under unloading normal stress. International Journal of Rock Mechanics and Mining Sciences, 114, 186-194. https://doi.org/10.1016/j.ijrmms.2019.01.003.

Figures

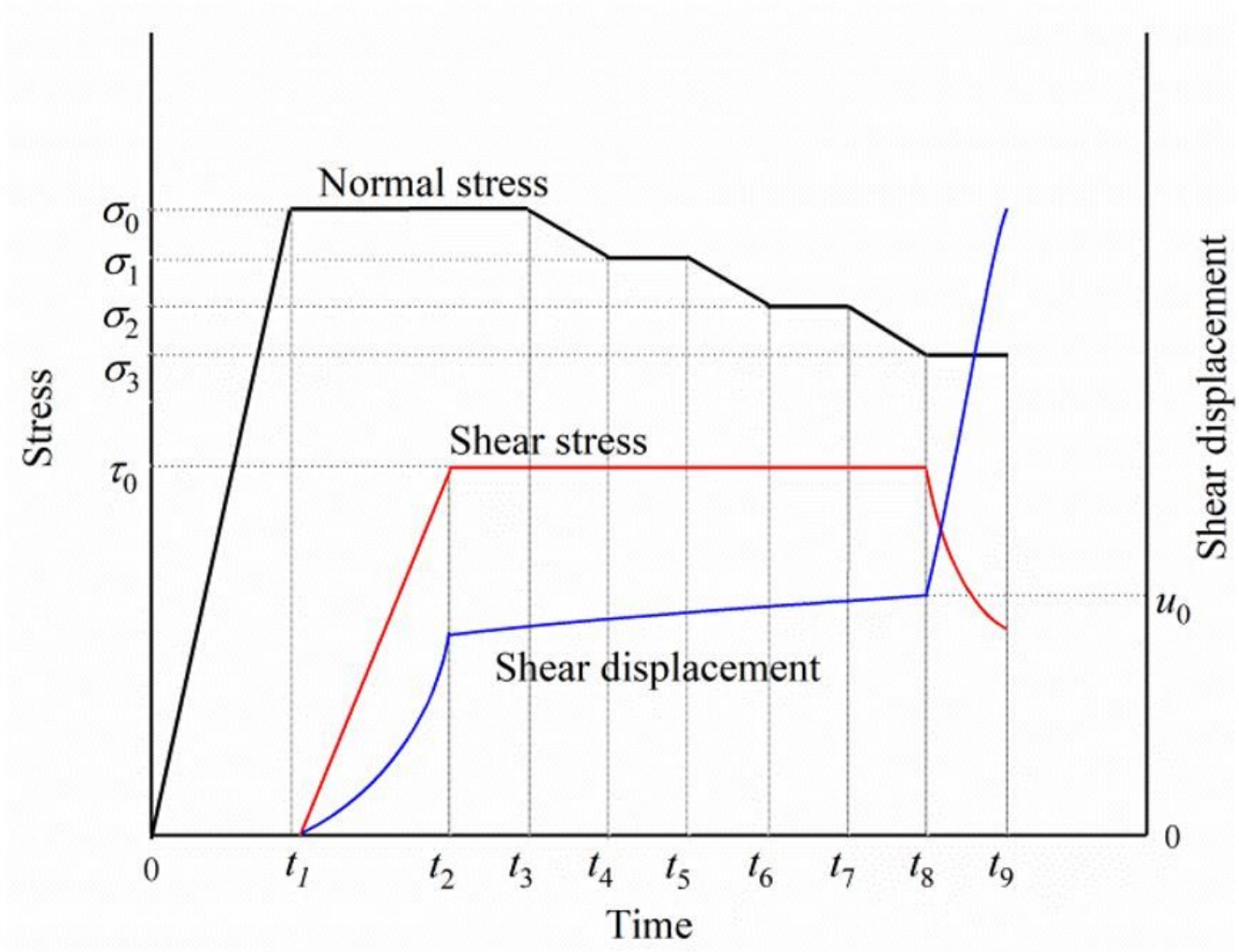

Figure 1

Stress paths of the normal stress unloading tests

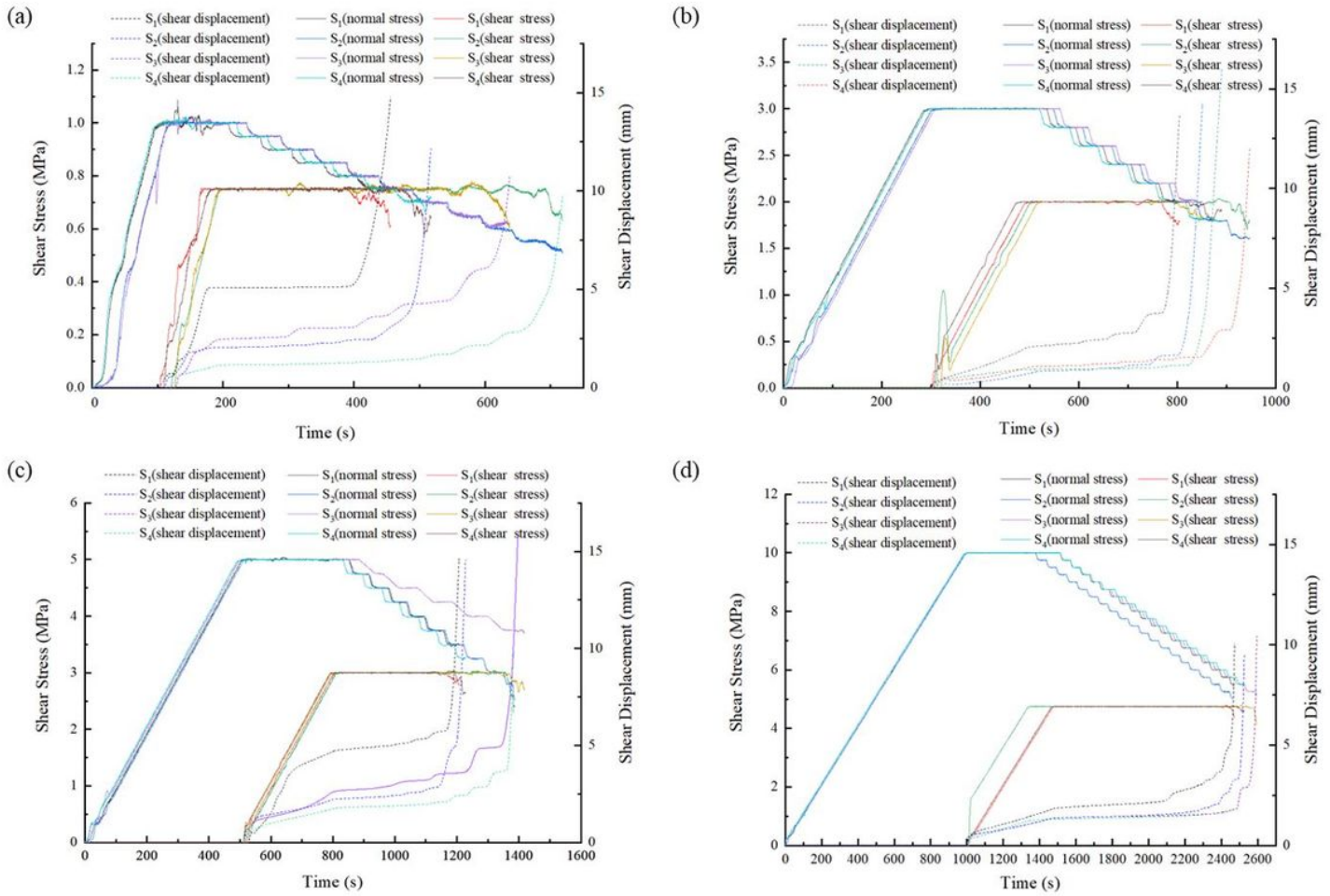

Figure 2

Typical Time-history curves of stress and displacement during the unloading of initial normal stress: (a) normal stress=1.0 Mpa; (b) normal stress=3.0 Mpa; (c) normal stress=5.0 Mpa; (d) normal stress=10.0 Mpa

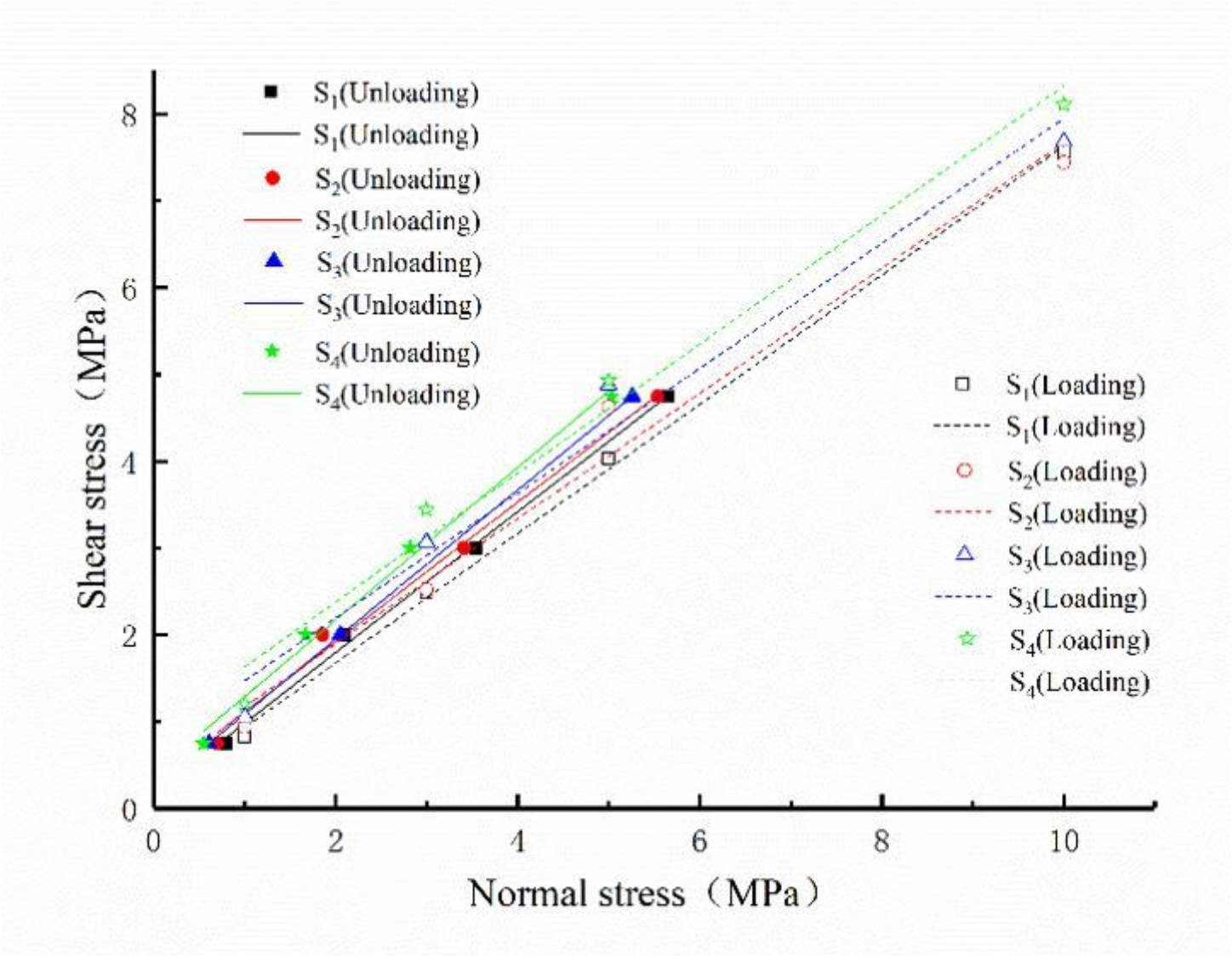

Figure 3

Relationship between normal stress and shear resistance

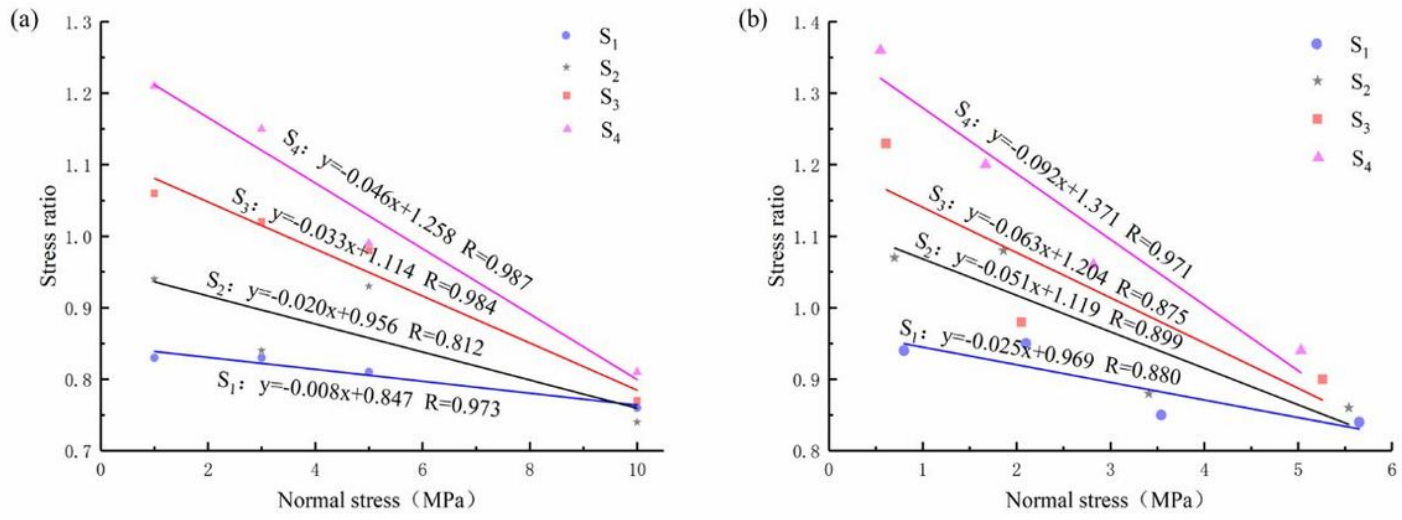

Figure 4

Linear regression of the stress ratios: (a) Tangential loading tests; (b) Normal unloading tests In order to intuitively compare the variations in stress ratios and reveal the unloading effect, the regression lines were plotted in one coordinate system, as shown in Fig.5

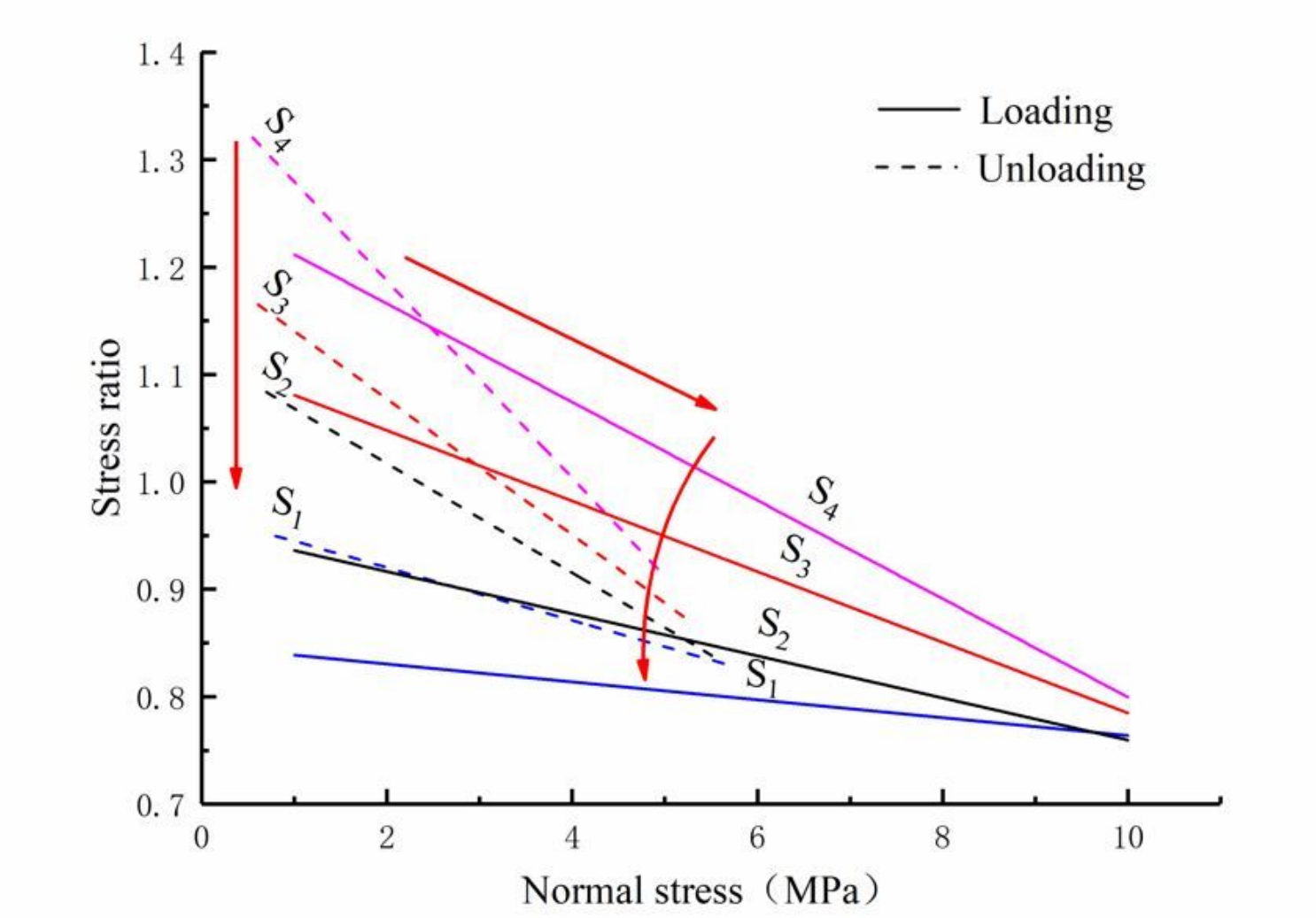

Figure 5

Comparison of loading and unloading curves

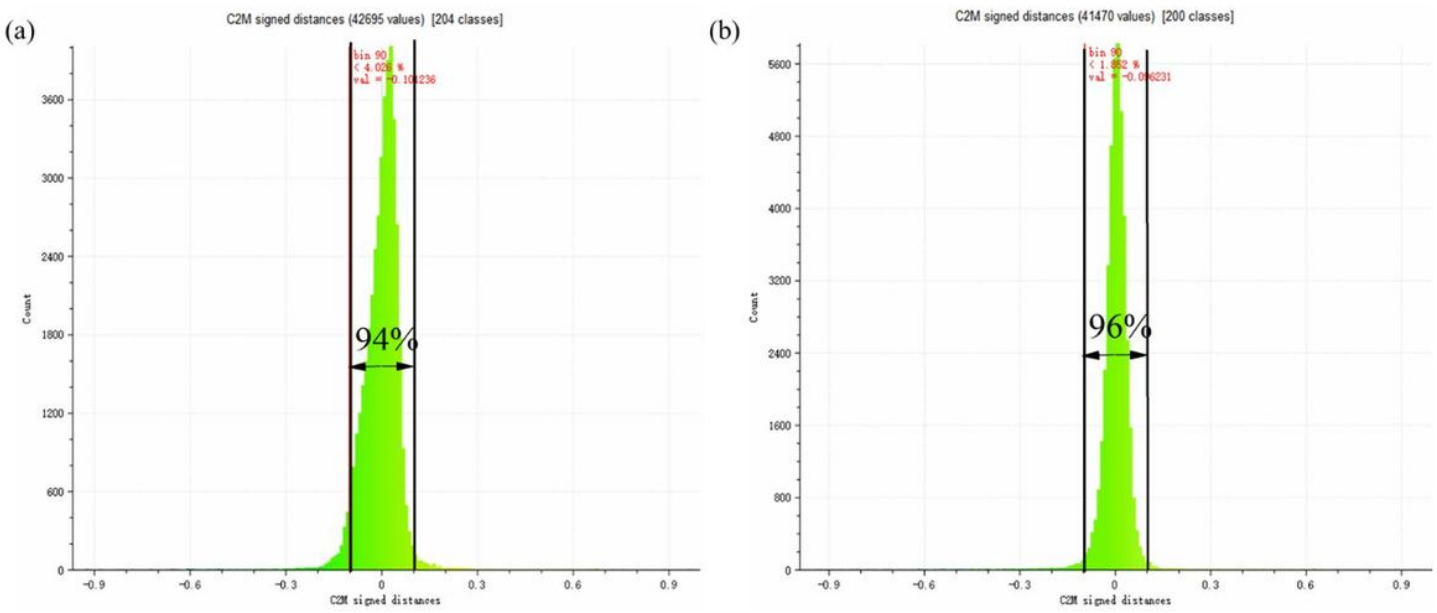

Figure 6

Comparison of point cloud data before and after normal loading